JCTC Journal of Chemical Theory and Computation

Mechanistic Analysis of the Base-Catalyzed HF Elimination from 4-Fluoro-4-(4′-nitrophenyl)butane-2-one Based on Liquid-Phase Kinetic Isotope Effects Calculated by Dynamics Modeling with Multidimensional Tunneling†

Yongho Kim,[§,II] Aleksandr V. Marenich,[II] Jingjing Zheng,[II] Kyung Hyun Kim,[§] Magdalena Kołodziejska-Huben,[‡] Michał Rostkowski,[‡] Piotr Paneth,*[,‡] and Donald G. Truhlar*[,II]

Institute of Applied Radiation Chemistry, Technical University of Lodz, Zeromskiego 116, 90-924 Lodz, Poland, Department of Chemistry, Kyung Hee University, Yongin-City, Gyeonggi-Do 449-701, Korea, and Department of Chemistry and Supercomputing Institute, University of Minnesota, 207 Pleasant Street SE, Minneapolis, Minnesota 55455-0431

Received August 20, 2008

Abstract: The primary and secondary deuterium kinetic isotope effects as well as leaving-group fluorine kinetic isotope effects have been calculated for the base-promoted elimination of hydrogen fluoride from 4-fluoro-4-(4′-nitrophenyl)butane-2-one in 75% aqueous methanol solution. The elimination was studied for both formate and imidazole as the catalytic base; and reactant and transition state structures and vibrational frequencies have been calculated by including the base explicitly and by including the solvent by an implicit solvation model that includes both electrostatics by class IV charges and first-solvation-shell effects by atomic surface tensions. We used the M06-L density functional for all calculations. The optimized stationary points, the geometry changes along the solution-phase minimum free energy path, and the solution-phase free energy profile indicate that the elimination reaction occurs concertedly but asynchronously via an E1cb-like transition state. Reaction rates were calculated by the equilibrium solvation path method, using variational transition state theory with multidimensional tunneling. The primary deuterium kinetic isotope effects are calculated to be large: 1.67 and 5.13 for formate and imidazole, respectively. The corresponding C_4-secondary deuterium kinetic isotope effects are 1.044 and 1.044, and the leaving group fluorine kinetic isotope effects are respectively 1.020 and 1.015.

Introduction

Enzymes often catalyze proton transfer from the α-carbon of a carbonyl compound by an E1cB mechanism.[1] Shultz et al. found that such reactions can also be catalyzed by an antibody elicited against an ammonium-containing hapten;[2−4] in particular they found a rate enhancement of a factor of 8.8 (compared to the acetate-promoted reaction) for elimination of HF from 4-fluoro-4-(4′-nitrophenyl)butane-2-one (Scheme 1); they found primary H/D kinetic isotope effects (KIEs) of 3.7 and 2.35 for acetate catalysis and the catalytic antibody, respectively. These KIEs rule out the E1 mechanism, in which a rate-limiting detachment of the leaving group precedes a fast proton-transfer step, but the results are consistent with the rate-limiting proton transfer occurring via either a concerted E2 or a stepwise E1cB mechanism.

* Corresponding author e-mail: paneth@p.lodz.pl (P.P.) and truhlar@umn.edu (D.G.T.).

† We dedicate this contribution to Hans-Heinrich Limbach on the occasion of his 65th birthday.

‡ Technical University of Lodz.

§ Kyung Hee University.

II University of Minnesota.

10.1021/ct800345j CCC: $40.75
Published on Web 12/04/2008

Scheme 1

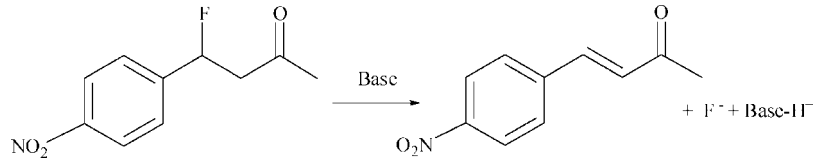

Scheme 2

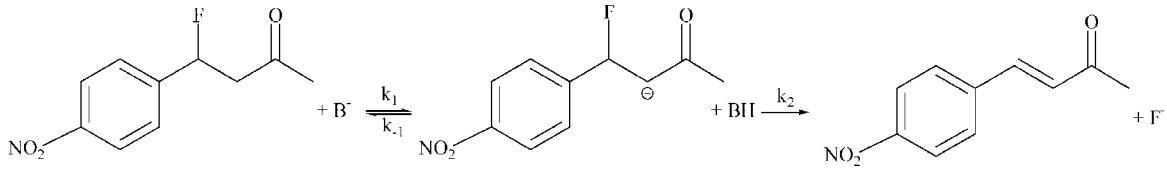

The study of secondary KIEs for such reactions can provide better discrimination between E2 and E1cB mechanisms, as discussed by Saunders[5,6] in conjunction with theoretical fluorine KIEs on model E2 and E1cB elimination reactions.

Based on experimental determinations of primary and secondary deuterium KIEs, and small fluorine KIEs for a set of bases with varying pK_a strengths (formate, acetate, and imidazole) in 75% aqueous methanol solution, Ryberg and Matsson argued that this reaction proceeds via either an E1cB mechanism (Scheme 2) or E1cB-like E2 mechanism.[7] The secondary deuterium KIEs in this study were at position C_4 (atom numbering is illustrated in Figure 1). In the subsequent work, based on deuteration at C_1 and C_3 and the measurement of multiple KIEs, they concluded, based on double isotopic fractionation[8] experiments, that the reaction proceeds by an E1cB mechanism.[9] However their analysis ignores tunneling and variational effects on the location of the transition state. In this respect, we note that the position of the variational transition state of the proton transfer reaction can be different from that of the deuteron transfer case, and furthermore multidimensional tunneling probabilities can be sensitive to secondary substitutions. Ryberg and Matsson's experimental values of the KIEs for the formate and imidazole cases are collected in Table 1, and the present paper will provide theoretical calculations of these values and of other details of the reaction in order to try to understand the mechanistic implications of the KIEs.

Reactions involving charge transfer or charged reactants or products provide an especially difficult challenge to theory because the effects of solvation can be very large.[10−21] Some of us have recently studied[22,23] the ability of electronic structure theory incorporating an implicit solvent, in particular the SM5.42/HF/6−31G(d) model,[24−28] to make reliable predictions of carbon, nitrogen, and oxygen KIEs on the decarboxylation of 4-pyridylacetic acid; however, we were unable to draw definitive conclusions. In later work it was demonstrated that several diverse computational levels cannot theoretically reproduce the experimental KIEs on a simple S_N2 reaction.[29−32] Therefore, it is important to carry out additional studies that allow us to understand the limits of reliability of theoretical KIEs for organic reactions, especially those involving polar or charged reagents. The wealth of experimental data for the title reaction prompts us to test the applicability of theoretical evaluations of KIEs for these elimination reactions, and that is the subject of the present article.

Computational Methods

The first decision to make is the representation of the potential energy surface. We decided to use density functional theory with an implicit solvation model because that is a cost efficient choice for reactions of complex molecules. We chose the M06-L density functional[33] because it is the most accurate available density functional without nonlocal exchange, and local density functionals are less computationally expensive than nonlocal ones for large systems. The present system is large enough that this savings is significant. Furthermore, we have developed an efficient and reasonably accurate implicit universal solvation model, called SM8,[35] that can be used with this functional in general organic solvents. Therefore all electronic structure calculations were carried out with the M06-L density functional and the SM8 solvation model. Furthermore we used the 6−31B(d) basis set[34] because this basis set has slightly more diffuse valence basis functions than the popular 6−31G(d) basis set, and it is therefore possibly more accurate for anions, especially for density functional theory calculations, which are more sensitive than wave function theory to the inclusion of diffuse

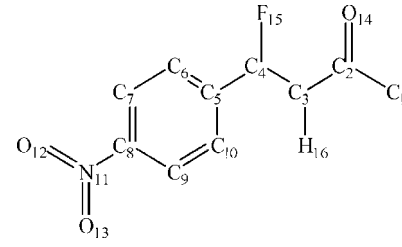

Figure 1. Numbering of atoms in the reactant.

Table 1. Experimental KIEs at 311 K

base	$(^{H}k/^{D}k)_s$[a,b]	$^{H}k/^{D}k$	$^{18}k/^{19}k$[b]
$HCOO^-$	1.038 ± 0.013 (1.009 ± 0.018)	3.2 ± 0.1	1.0037 ± 0.0020
$C_3H_4N_2$	1.014 ± 0.017 (1.010 ± 0.023)	7.5 ± 0.1	1.0013 ± 0.0012

[a] Values not in parentheses are secondary deuterium KIE of hydrogen at C_4. [b] Values in parentheses were obtained for the reactant perdeuterated in positions 1 and 3.

basis functions. In the SM8 calcuations, we used the CM4 M charge model,[36] which has been shown to be much more accurate and much more stable than using population analysis for the solute partial charges. All electronic structure calculations were carried out using the MN-GFM[37] and MN-GSM[38] modules incorporated locally into the *Gaussian03* electronic structure program.[39]

All stationary point geometries were fully optimized in the reaction field of the implicit solvent. Vibrational analysis was performed for each stationary point based on analytical gradients and numerical Hessians. All minima and transition states (TSs) were confirmed to have zero and one imaginary frequency, respectively, and Hessians from these calculations were used for calculations of KIEs by variational[40−42] transition state theory. Since experimentally the reaction was carried out in a binary methanol-water mixture (3:1 v/v), all the parameters used with the solvation models were interpolated linearly from the values for pure solvents. The resulting dielectric constant equals 44.05. Although the rate constants are calculated at 311 K, we used solvation parameters corresponding to 298 K.

We were unable to obtain a stable intermediate structure as shown in Scheme 2 for reaction involving either base at the chosen level of electronic structure theory. Every attempt to locate an intermediate led to C−F bond breaking to generate 4-(4′-nitrophenyl)butene-2-one and fluoride ion. The calculations therefore predict a concerted E2 mechanism. Furthermore, as discussed in more detail below, the conventional transition state has the proton or deuteron partially transferred with the fluoride bond almost intact. Thus the mechanism may be labeled as E1cb-like E2.

The reaction rates of the E2 reaction have been calculated using variational transition state theory[40−42] including a transmission coefficient[43−47] that accounts for multidimensional tunneling. The solvation effects were calculated in the equilibrium solvation path (ESP) approximation,[14] and all rate calculations were carried out by direct dynamics[48−50] with the interpolated variational transition state theory by mapping[51] (IVTST-M) algorithm using the *Gaussrate*[52] program, which is an interface of *Gaussian03*[39] and the *Polyrate*[53] dynamics program.

In the ESP approximation,[14] the stationary points along the minimum free energy path (which we abbreviate, by analogy to the minimum-energy path for gas-phase reactions, as MEP) are calculated in the liquid phase. The MEP corresponds to the path of steepest descent in isoinertial solute cooordinates on a $(3N-6)$-dimensional potental of mean force (where N is the number of atoms in the solute, that is, the total number of atoms in the saddle point structure) called V_2 or U in ref 14; we will call it U. It is evaluated in the zero-order canonical mean shape (CMS-0) approximation.[14,47] In this approximation, U is obtained by adding the gas-phase potential energy of the solute to the standard-state free energy of solvation, and the saddle point on this solute free energy surface will be called the conventional transion state (TS). The signed distance from the TS along the MEP in isoinertial solute coordinate is called the reaction coordinate s. The variational transition state for a canonical ensemble at temperature T is located at the position on the MEP where the standard-state generalized free energy of activation $\Delta G(\mathrm{GT}, s|T)$ is a maximum, when $\Delta G(\mathrm{GT}, s|T)$ is obtained[14,47] by adding the local rovibrational free energy to U. In the present application the local rovibrational free energy consists of the local zero-point vibrational energy of the solute plus the local thermal rotational−vibrational free energy. All vibrational energies and vibrational free energies are computed harmonically from solution-phase frequencies. This yields the canonical variational theory (CVT) rate constant given by[14]

$$k^{\mathrm{CVT}} = \frac{k_B T}{hC^\circ}\exp[-\Delta G^{\mathrm{CVT},0}/RT] \qquad (1)$$

where k_B is the Boltzman constant; h is Planck's constant; C° is the concentration (1 molar) corresponding to the standard state; R is the gas constant; and $\Delta G^{\mathrm{CVT},0}$ is the standard state free energy of activation, which is the maximum along s of $\Delta G(\mathrm{GT}, s|T)$. Conventional transition state theory for a reaction in solution is not clearly defined by traditional treatments, but it is defined here as evaluating the rate constant at the s value that maximizes $U(s|T)$ rather than the one that maximizes $\Delta G(\mathrm{GT}, s|T)$; the variational effect is then defined as the diffference in rate constant due to the difference in the location of the two maxima. A reaction is especially susceptible to variational effects when $U(s|T)$ is rather flat near its maximum, when a reaction is asymmetric (so that the first derivative of the local rovibrational free energy with respect to s evaluated at the maximum of $U(s|T)$ is neither zero by symmetry nor small by near symmetry), or when one is considering higher temperatures (which increase the importance of entropic effects in $U(s|T)$ can also contribute to the local rovibrational free energy). However, these guidelines have their limtations, and one sometimes finds large variational effects even for symmetric reactions at low temperature or for reactions with barriers greater than 10 kcal/mol.

In order to include tunneling, $k^{\mathrm{CVT}}(\mathrm{T})$ is multiplied by a transmission coefficient, κ^{SCT}.

$$k^{\mathrm{CVT/SCT}}(\mathrm{T}) = \kappa^{\mathrm{SCT}}(\mathrm{T})k^{\mathrm{CVT}}(\mathrm{T}) \qquad (2)$$

The transmission coefficient is defined as the ratio of the thermally averaged quantal transmission probability, $P(\mathrm{E})$, to the thermally averaged classical transmission probability for the effective vibrationally adiabatic potential energy along the reaction coordinate.[43,47] The effective vibrationally adiabatic potential energy for the tunneling calculation will be called V_a (it is called V_2 in ref 14); V_a, like U, is calculated in the CMS-0 approximation.[14,47] In this appproximation, the one-dimensional V_a is equal to U plus the local solute zero-point energy along the MEP. (This should not be confused with the one-dimensional generalized free energy of activation profile.) The centrifugal-dominant small-curvature semiclassical adiabatic ground state (CD-SCSAG) tunneling approximation[46,54] was used to calculate $P(\mathrm{E})$; this is called small-curvature tunneling (SCT) for conciseness.

In the IVTST-M algorithm for a solution-phase reaction, the necessary information (free energies, free energy gradients, and free energy Hessians) for the CVT/SCT calculation is computed at a small number of points along the minimum

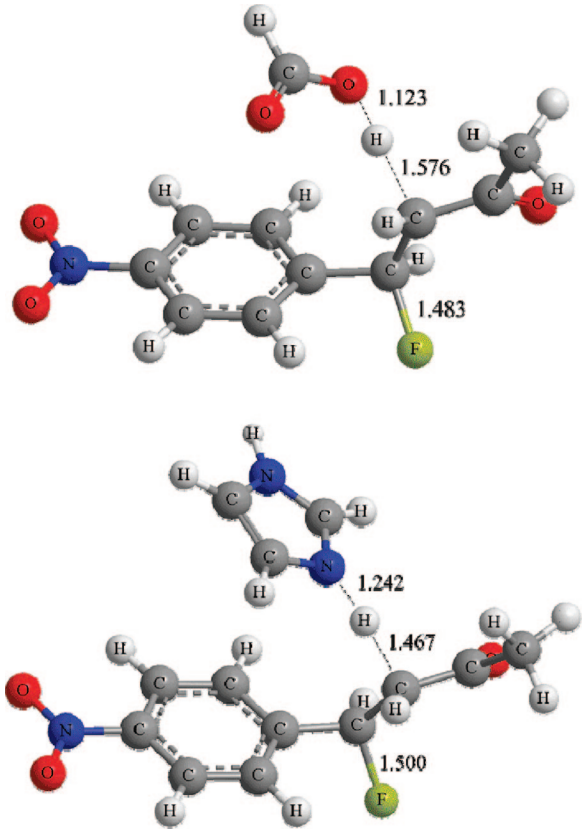

Figure 2. The conventional TS structures for the proton abstraction by formate and imidazole bases calculated at the SM8/CM4M/M06-L/6−31B(d) level.

energy path and fitted to spline functions under tension. We use the notation[51] IVTST-M−*H/G* to denote the number of nonstationary points at which Hessians (*H*) and free energies and gradients (*G*) are calculated. The reaction coordinate for each of the isotopomers was obtained by the RODS algorithm.[51,56]

Results and Discussion

The conventional transition state (TS) structures in solution for the proton abstraction by formate and imidazole bases calculated at the SM8/CM4M/M06-L/6−31B(d) level are illustrated in Figure 2. The imaginary frequencies at the TS are 896i and 1199i cm^{-1} for the reactions with formate and imidazole bases, respectively.

We were able to optimize the intermediate structures successfully in the absence of solvent but were unable to optimize them in solution either with or without the bases. When this was attempted, the C_4−F bond was always broken to generate fluoride ion, which is reasonable since the solvation energy for a small ion is large in a polar solvent. This means that the reaction in solution is concerted at the employed level of electronic structure theory. In terms of the reaction mechanism, it is important to know whether the intermediate is present or not, so further studies to corroborate this prediction would be worthwhile. However, if we assume it is not present, then this reaction becomes an example of the merging[57,58] of the stepwise and concerted mechanisms by the disappearance of the intermediate.

Table 2. Calculated Bond Lengths (Å) and Mayer's Bond Orders for Stationary Points in the Gas Phase and in Solution[a]

	reactants	conventional TS	intermediate	products
		Formate Base		
C_3−H	1.100/*1.100*	1.576/*1.627*	*1.787*	-
	(0.835/*0.895*)	(0.334/*0.333*)	(*0.262*)	
C_4−F	1.415/*1.392*	1.483/*1.451*	*1.456*	-
	(0.501/*0.518*)	(0.454/*0.471*)	(*0.466*)	
C_3−C_4	1.512/*1.516*	1.467/*1.467*	*1.463*	1.349/*1.348*
	(0.937/*0.943*)	(1.046/*1.043*)	(*1.066*)	(1.730/*1.748*)
O−H	-	1.123/*1.102*	*1.049*	0.983/*0.976*
		(0.336/*0.349*)	(*0.426*)	(0.667/*0.706*)
		Imidazole Base		
C_3−H	1.100/*1.100*	1.467/*1.748*	*2.105*	-
	(0.835/*0.895*)	(0.235/*0.355*)	(*0.221*)	
C_4−F	1.415/*1.392*	1.500/*1.400*	*1.398*	-
	(0.501/*0.518*)	(0.472/*0.472*)	(*0.477*)	
C_3−C_4	1.512/*1.516*	1.469/*1.509*	*1.501*	1.349/*1.348*
	(0.937/*0.943*)	(1.038/*0.960*)	(*0.985*)	(1.730/*1.748*)
N−H	-	1.242/*1.127*	*1.055*	1.015/*1.014*
		(0.169/*0.352*)	(*0.507*)	(0.672/*0.693*)

[a] The gas phase values are in italic, and the numbers in parentheses are Mayer bond orders.

Geometric parameters and bond orders for stationary points optimized in the gas phase at the M06-L/6−31B(d) level and in solution by SM8/CM4M/M06-L/6−31B(d) are given in Table 2. Table 2 lists bonds that undergo major changes in the course of the reaction. These include the C_3−H and the O−H (N−H in case of imidazole) bonds, which are broken and formed, respectively, along with the C_4−F bond that is broken in the reaction and the C_3−C_4 bond that becomes a double bond. The corresponding bond orders calculated by the method of Mayer[59] are given in parentheses. Note that the Mayer bond order is calculated from the reference Slater determinant of the density functional calculation, and this is preferred to the Pauling bond order,[60] which is a function only of distance.

Customarily, the analysis of the position of the TS is carried out in terms of its synchronicity and looseness. A transition state is considered synchronous if the bond breaking is as advanced as bond making[61] (often also it is assumed that the total bond order to the central atom is preserved[62]). If the sum of the bond orders to the transferred atom is diminished or increased, the corresponding transition state is called loose or tight, respectively.[61,63] Table 2 shows that in the gas phase the bond order sum of the transferred hydrogen changes from about 0.90 in the reactant to about 0.69 in the intermediate for the formate base reaction and from 0.90 to 0.73 for the imidazole base reaction. The average of these values is 0.80 for formate and 0.82 for imidazole. Table 2 shows that the sum of the hydrogen bond orders at the TS is 0.68 of formate and 0.72 for imidazole. Since these are slightly smaller than the averages mentioned earlier, they indicate a slightly exploded (loose) transition state for the proton transfer step in the gas phase. The same is true for the reactions in solution; in particular, the total bond order at the TS of the imidazole base reaction is only 0.40, which makes it a very loose and polar transition state.

In the gas phase, the reaction mechanism is E1cB, that is, a two-step mechanism. The first step, from reactants to an

Table 3. Calculated Partial Atomic CM4M Charges in Solution and in the Gas Phase at the M06-L/6-31B(d) Level of Theory[a]

		conventional TS		intermediate	
atom	reactants	formate	imidazole	formate	imidazole
C_2	0.35(0.28)	0.31(0.21)	0.27(0.17)	(0.20)	(0.14)
C_3	−0.17(−0.15)	−0.45(−0.29)	−0.31(−0.29)	(−0.29)	(−0.27)
O_{14}	−0.51(−0.36)	−0.58(−0.47)	−0.59(−0.50)	(−0.48)	(−0.52)
F_{15}	−0.25(−0.21)	−0.34(−0.30)	−0.36(−0.23)	(−0.31)	(−0.22)
H_{16}	0.14(0.10)	0.30(0.30)	0.33(0.29)	(0.30)	(0.30)
O_F	−0.59(−0.59)	−0.45(−0.44)	-	(−0.41)	-
N_I	−0.56(−0.44)	-	−0.44(−0.36)	-	(−0.34)

[a] Numbers in parentheses are for the gas phase. Oxygen (O_F) and nitrogen (N_I) atoms are in formate and imidazole, respectively.

intermediate, is rate limiting. The C_3−H bond at the conventional TS of the first step of the formate base reaction has a bond order of 0.33 in the gas phase, which is 89% of the way to the intermediate, and the O−H bond has a bond order of 0.35, which is 82% of its bond order at the intermediate. This indicates that the TS is very late (product-like; the product is an intermediate in this case). In solution, where there is no intermediate, the C_3−H and O−H bond orders at the TS are 0.33 and 0.34, which have changed 60% and 50%, respectively, of their total change in going all the way to products. Therefore the TS in solution is nearly synchronous or slightly late, which is consistent with the change of C_3−H and N/O−H bond lengths between the gas phase and the solution transition states. In contrast the C_3−H and N−H bond orders at the TS of the imidazole base reaction are 0.24 and 0.17, which have changed 72% and 25%, respectively, of their total change in going all the way to products. This analysis of the transition state is most useful when the bond order is approximately preserved in the course of the reaction. If the transition state is very loose or tight, the bond orders for breaking and forming bonds at the TS are very small or large, respectively. In this case the earliness and lateness of the TS does not provide such useful information. Experimentally this analysis of TS character is performed using the α-secondary H/D kinetic isotope effect, which often primarily reflects the changes in the force constant of secondary C−H bonds at the TS. The α-secondary H/D KIE may be a better tool to compare the similarity of the TS with reactants or products than the bond orders of the hydrogen that is being transferred.

As illustrated by the data collected in Table 3 changes in partial charges are primarily concentrated in the reacting fragment of the molecule. The changes in the partial charges of C_2, C_3, and O_{14} from the reactant to the intermediate in the gas phase show that the intermediate has a fairly large enolate character, and the partial charges of the TS in the gas phase are very similar to those of intermediates, which is consistent with the late (enolate-like) transition state. All partial charges of the TS in solution are larger than the corresponding values in the gas phase.

Energetic data for two of the bases are collected in Table 4. For the table, zero of energy is the potential energy of reactants, that is, 4-fluoro-4-(4′-nitrophenyl)butane-2-one infinitely separated form bases. The energy differences between the gas-phase TSs and intermediates are very small, which is also consistent with the late transition state in the gas phase. The solvent effect reduces the barrier height of the imidazole base reaction by about 4 kcal/mol.

Table 4. Energetics of Stationary Points (in kcal/mol)

	gas-phase *V*			solution-phase *U*		
base	R[a]	TS	Int	R[b]	TS	effective barrier[c]
$HCOO^-$	0	−19.3[d]	−19.4	−92.4	−73.0	19.4[c]
$C_3H_4N_2$	0	20.8	19.8	−26.7	−10.2	16.5

[a] Gas-phase reactants, taken as zero of energy for next columns. [b] Solution-phase reactants. [c] *U*(TS) − *U*(R). [d] In the gas phase there is an ion-dipole complex between R and TS; the energy of the TS for $HCOO^-$ is lower than that of the reactant but higher than that of the ion-dipole complex.

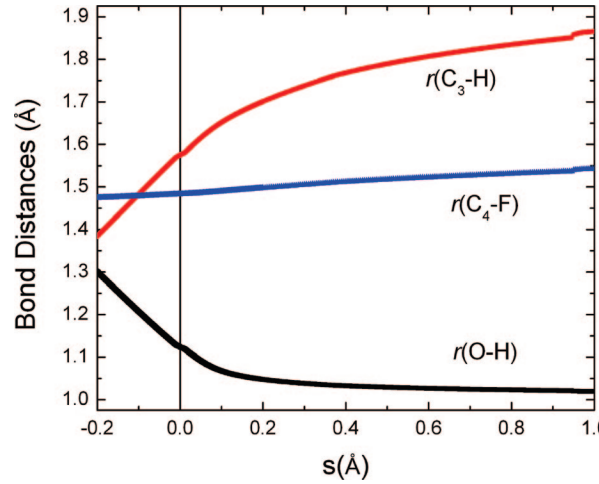

Figure 3. Bond distances along the reaction coordinate for the formate base reaction in solution. The vertical line is at the conventional TS. Negative and positive *s* values represent respectively the reactant side (before transion state) and the product side (after transition state) of the reaction paths.

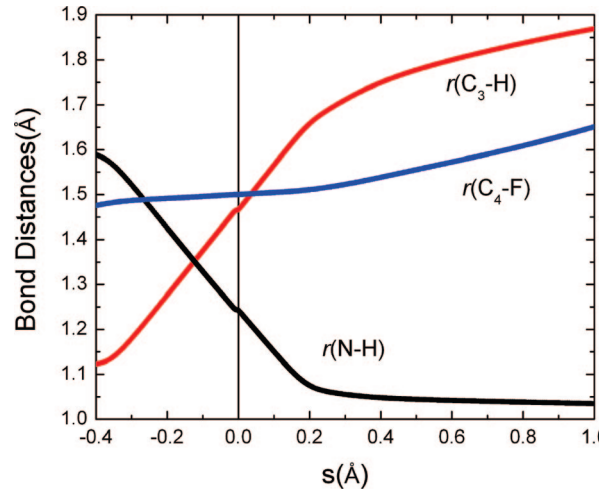

Figure 4. Bond distances along the reaction coordinate for the imidazole base reaction in solution. The vertical line is at the conventional TS. Negative and positive *s* values represent the reactant side and the product side of reaction paths, respectively.

The changes in some geometric parameters along the solution-phase MEP are illustrated in Figures 3 and 4 for the formate and imidazole base reactions, respectively, where *s* is the signed distance along the MEP (with the TS defining $s = 0$) in isoinertial coordinates scaled to a mass of 1 amu.

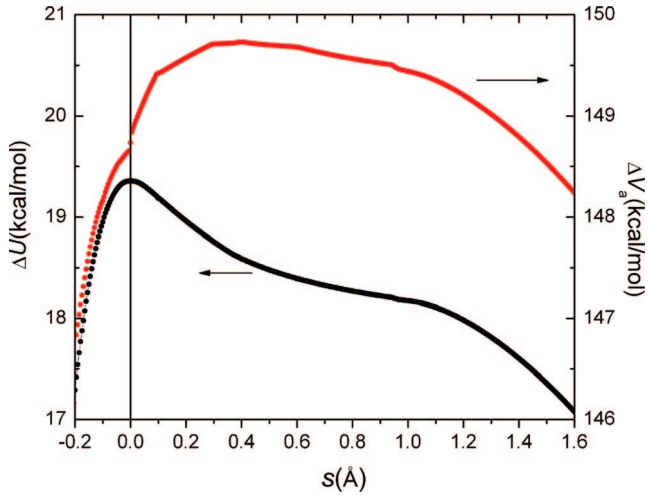

Figure 5. Potential of mean force and vibrationally adiabatic effective potential energy along the reaction coordinate of the HF elimination with formate base calculated by the IVTST-M method. Both curves in the figure are relative to reactants. The vertical line is at the conventional TS. Seven nonstationary Hessian ($s = -0.2$, -0.1, 0.1, 0.3, 0.4, 0.6, 0.95 Å) and 244 energy and gradient points were used [IVTST-M-7/244].

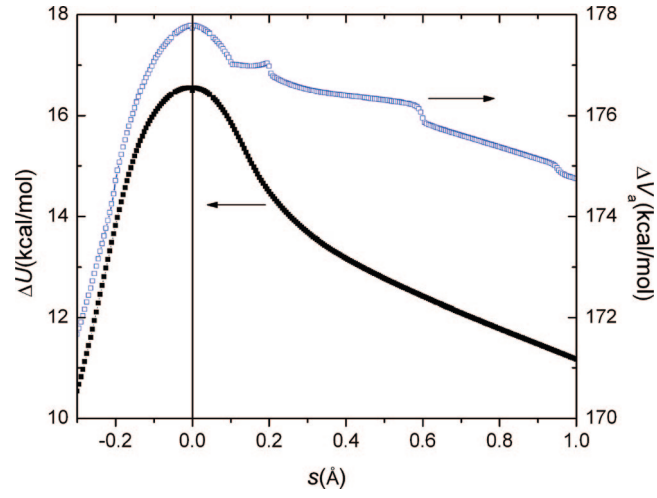

Figure 6. Potential of mean force and vibrationally adiabatic effective potential energy along the reaction coordinate of the HF elimination with imidazole base calculated by the IVTST-M method. Both curves in the figure are relative to reactants. The vertical line is at the conventional TS. Eight nonstationary Hessian ($s = -0.2$, -0.1, -0.05, 0.05, 0.1, 0.2, 0.6, 0.95 Å) and 283 energy and gradient points were used [IVTST-M-8/283].

As shown in Figure 3, the values of the C_3-H and O−H bond lengths cross before the reaction proceeds to a point at $s = -0.2$ Å. At the TS, the O−H distance is much shorter than the C_3-H distance, which is consistent with the late transition state in terms of the proton abstraction. Most of the proton transfer is finished before the point at $s = 0.2$ Å on the reaction path. However the C_4-F distance does not change much in the region of reaction coordinate shown in Figure 3. The bond distances in the imidazole base reaction, as illustrated in Figure 4, are changed in a similar way, except that the point where the C_3-H and O−H bond cross is slightly closer to the TS. Likewise, the transition state is late. Interestingly, the C−F bond length increases more rapidly after the proton transfer is almost finished at $s = 0.2$ Å. These results suggest that the elimination of HF from 4-fluoro-4-(4′-nitrophenyl)butane-2-one occurs asynchronously in a concerted mechanism, E2, with an E1cB-like transition state.

The proton is transferred first and followed by C−F bond cleavage without any intermediate. Specific solvent effects such as hydrogen bonds between solute and hydroxylic solvent are not considered explicitly in this study although to some extent they are implicit in the SM8 solvation model, so further study would be necessary to elucidate their role in the mechanism.

The generalized free energy of activation profile and the vibrationally adiabatic energy curves along the reaction coordinate are illustrated in Figures 5 and 6 for the formate and imidazole base reactions in solution, respectively. In both reactions, the free energies on the reactant side (negative s values) decrease very rapidly as the system leaves the TS, whereas the product side (positive s values) free energies are reduced slowly. In addition, the vibrationally adiabatic energy curve for the elimination by formate is very flat and wide near its maximum at $s = 0.4$ Å. The free energy of activation profiles at 311 K are qualitatively similar in shape to the vibrationally adiabatic curves. As a consequence there is a large variational effect (i.e., a large difference of CVT from conventional TST) for formate, but the variational effect for imidazole is less than 3% for any of the isotopomers studied. For formate the variational transition state is 0.41 Å later than the conventional TS for the all-protium case and 0.62 Å later than the conventional TS for dideuterium substitution at C-3. The variational effect lowers the rate coefficient by a factor of 6.2 for the all-protium case and a factor of 2.2 for dideuterium substitution at C_3. The resulting primary KIEs are shown in Table 5.

Table 5. Calculated Primary H/D KIEs and Ratios of Transmission Coefficients at 311 K[a]

base	k^{TST}	k^{CVT}	κ^{SCT}	$k^{CVT/SCT}$
formate	4.60	1.62	1.02	1.67
imidazole	5.29	5.29	0.97	5.13

[a] Each quantity in the table is the ratio of the values for all-protium HF elimination to that for dideuterium substitution at C_3. TST denotes conventional TS theory.

Table 6. Secondary KIEs and Ratios of Transmission Coefficients at 311 K

	secondary H/D[a]				$^{18}F/^{19}F$			
base	k^{TST}	k^{CVT}	κ^{SCT}	$k^{CVT/SCT}$	k^{TST}	k^{CVT}	κ^{SCT}	$k^{CVT/SCT}$
formate	0.943	1.045	0.999	1.044	1.005	1.021	1.001	1.020
	0.943	1.035	0.997	1.046				
imidazole	1.012	1.014	1.030	1.044	1.006	1.007	1.008	1.015
	1.012	1.012	1.012	1.024				

[a] The upper entry is for D substitution at C_4; the lower entry is for perdeuterated reactants.

We also calculated the secondary deuterium KIEs and the primary fluorine KIEs, and these are in Table 6. Again we see large variational effects for formate. The deuterium KIEs are in better agreement with experiment (see Table 1) than are the fluorine KIEs. For example, for formate, the

experimental result is 0.4% and the simulation gives 2.0%. So evidently something is missing in the theoretical description of these reactions. Perhaps there is another step that is partly rate determining and which does not introduce isotopic fractionation. What the experimental KIEs would seem to be telling us is maybe that most rate limiting hydrogen transfers occur with minor contributions from C−F bond breaking, but if we accepted that interpretation, then the small value of the primary deuterium KIE for formate cannot be explained. So we tentatively base our interpretation mainly on the larger KIEs.

Matsson and co-workers[9] have also provided further interpretation of the KIEs reported in Table 1. The secondary KIEs that they determined for the reactant perdeuterated in positions 1 and 3 are smaller than those for the isotopomers that have protium at these positions; they ascribed this to a mechanistic effect, namely the differences to changes in the commitment on rate constants k_2 and k_{-1} caused by the deuterium KIEs. In their analysis they assumed that the first step of the proton transfer does not exhibit any sizable fluorine KIE. Based on these results they postulated that the reaction proceeds by the E1cb mechanism. Our calculated primary H/D KIEs and ^{18}F/^{19}F KIEs are slightly smaller and larger, respectively, than the corresponding experimental results. The transmission coefficients, κ^{SCT}, for formate and imidazole promoted reactions without isotopic substitutions are 1.06 and 3.50 at 311 K, respectively. The small transmission coefficient for the formate reaction is attributed to the flat effective vibrationally adiabatic potential curve as shown in Figure 5. The tunneling contribution to the KIE, which is the ratio of transmission coefficient of the natural isotopomer to that of the substituted isotopomer, is almost unity for both reactions. The isotopic substitution does not change the tunneling coefficient much in these reactions. The secondary H/D KIEs agree better with experimental values. Interestingly the quasiclassical secondary H/D KIEs, which are from the rate constants without tunneling (that is, from k^{CVT}), become smaller when perdeuterated reactants are used, which means that the small secondary KIEs in experiment using the perdeuterated reactants may not be caused by the change in the commitment of stepwise processes. The smaller KIEs may be just an outcome of the zero-point and thermal vibrational energy changes at the transition state, so they cannot be used as evidence of the stepwise mechanism. The equilibrium secondary H/D KIE is 1.20 for both formate and imidazole promoted reactions. Comparing this value with the quasiclassical secondary H/D KIEs implies early transition states in terms of the force constant change at the C-4 position. Together with our earlier discussion of the lateness of the transition state in terms of the partial charges and the C_3−H bond distances, we postulate that the proton transfer and the fluoride dissociation occur very asynchronously at the level of theory used in this study, and the TS is very similar to the intermediate of the E1cB mechanism if it exists.

Comparison of the results of our calculations with the experimental values led us to a different interpretation from that of Matsson and co-workers. We conclude that the results of the secondary deuterium KIEs and the primary fluorine KIEs indicate that experimentally measured values correspond directly to the intrinsic KIEs on the reaction. The dependence of the observed KIEs on deuteration is in all cases well inside the experimental errors and cannot therefore be conclusive. Our results are in agreement with Thibblin and Ahlberg's[64] suggestion that the secondary leaving group fluorine KIE may also appear on the deprotonation process in the elimination reaction; they ascribed this effect to negative ion hyperconjugation. This was further supported by Saunders' calculations[65,66] of KIEs of the leaving group. Our calculations indicate that the bond order of the C_4−F bond decreases from 0.52 to 0.47 for both formate and imidazole promoted reactions in solution.

The results of the primary deuterium KIEs are also in agreement with the above interpretation, although the quantitative accuracy of the theoretical prediction of these KIEs is lower than of the other two. The size of the primary deuterium KIEs on proton transfer is considered to be a measure of the synchronicity of the transition state. The maximal primary KIE is expected for the most synchronous transition state,[61,67] the situation that occurs when the donor and the acceptor are of equal pK_a. It is interesting to note that in the present case the dependence is opposite; the smallest difference in pK_a is for the imidazole, which is characterized by the largest primary deuterium KIE; however, as mentioned above, the transition state for this reaction is less synchronous than the other.[58] This imbalance deserves further investigations.

Conclusions

We have used M06-L/6−31B(d) level of electronic structure theory with the SM8 solvation model, the CM4M charge model, and CVT/SCT dynamical theory in the equilibrium solvation path approximation to study KIEs on the base promoted elimination of HF from 4-fluoro-4-(4′-nitrophenyl)-butane-2-one. Our results indicate a concerted mechanism with an E1cB-like transition state and highly asynchronous processes for the proton transfer and fluoride dissociation. The tunneling contribution to the KIEs is very small due to very flat effective adiabatic potential energy curves near the transition state.

Acknowledgment. The authors are grateful to Yan Zhao for helpful discussions. These studies were supported by research grants from the State Committee for Scientific Research (KBN Poland) and by the National Science Foundation under Grant No. CHE07-04974. Y. Kim appreciates the financial support in part from the Kyung Hee University.

References

(1) Gerlt, J. A.; Gassman, P. G. *J. Am. Chem. Soc.* **1992**, *114*, 5928.

(2) Shokat, K. M.; Leumann, C. J.; Sugasawara, R.; Schultz, P. G. *Nature* **1989**, *338*, 269.

(3) Shokat, K. M.; Uno, T.; Schultz, P. G. *J. Am. Chem. Soc.* **1994**, *116*, 2261.

(4) Romesberg, F. E.; Flanagan, M. E.; Uno, T.; Schultz, P. G. *J. Am. Chem. Soc.* **1998**, *120*, 5160.

(5) Saunders, W. H., Jr. *J. Org. Chem.* **1997**, *62*, 244.

(6) Saunders, W. H., Jr. *J. Org. Chem.* **1999**, *64*, 861.

(7) Ryberg, P.; Matsson, O. *J. Am. Chem. Soc.* **2001**, *123*, 2712.

(8) Cleland, W. W. In *Enzyme Mechanism from Isotope Effects*; Cook, P. F., Ed.; CRC Press: Boca Raton, 1991; p 247.

(9) Ryberg, P.; Matsson, O. *J. Org. Chem.* **2002**, *67*, 811.

(10) Hwang, J.-K.; Creighton, S.; King, G.; Whitney, D.; Warshel, A. *J. Chem. Phys.* **1988**, *89*, 859.

(11) Sola, M.; Lledos, A.; Duran, M.; Bertran, J.; Abboud, J.-L. M. *J. Am. Chem. Soc.* **1991**, *113*, 2873.

(12) Assfeld, X.; Garapon, J.; Rinaldi, D.; Ruiz-Lopez, M. F.; Rivail, J. L. *THEOCHEM* **1996**, *371*, 107.

(13) Lee, I.; Kim, C. K.; Lee, B.-S.; Kim, C. K.; Lee, H. W.; Han, I.-S. *J. Phys. Org. Chem.* **1997**, *10*, 908.

(14) Chuang, Y.-Y.; Cramer, C. J.; Truhlar, D. G. *Int. J. Quantum Chem.* **1998**, *70*, 887.

(15) Lim, D.; Jenson, C.; Repasky, M. P.; Jorgensen, W. L. *ACS Symp. Ser.* **1999**, *721*, 74.

(16) Cramer, C. J.; Truhlar, D. G. *Chem. Rev.* **1999**, *99*, 2161.

(17) Naka, K.; Sato, H.; Morita, A.; Hirata, F.; Kato, S. *Theor. Chem. Acc.* **1999**, *102*, 165.

(18) McRae, R. P.; Schenter, G. K.; Garrett, B. C.; Svetlicic, Z.; Truhlar, D. G. *J. Chem. Phys.* **2001**, *115*, 8460.

(19) Gronert, S.; Pratt, L. M.; Mogali, S. *J. Am. Chem. Soc.* **2001**, *123*, 3081.

(20) Pliego, J. R., Jr. *J. Mol. Catal. A* **2005**, *239*, 228.

(21) Truhlar, D. G.; Pliego, J. R., Jr. In *Continuum Solvation Models in Chemical Physics*; Mennucci, B., Cammi, R., Eds.; Wiley: Chichester, 2008; p 338.

(22) Sicinska, D.; Paneth, P.; Truhlar, D. G. *J. Phys. Chem. B* **2002**, *106*, 2708.

(23) Sicinska, D.; Truhlar, D. G.; Paneth, P. *J. Am. Chem. Soc.* **2001**, *123*, 7683.

(24) Hariharan, P. C.; Pople, J. A. *Theor. Chim. Acta* **1973**, *28*, 213.

(25) Li, J.; Hawkins, G. D.; Cramer, C. J.; Truhlar, D. G. *Chem. Phys. Lett.* **1998**, *288*, 293.

(26) Li, J.; Zhu, T.; Hawkins, G. D.; Winget, P.; Liotard, D. A.; Cramer, C. J.; Truhlar, D. G. *Theor. Chem. Acc.* **1999**, *103*, 9.

(27) Zhu, T.; Li, J.; Liotard, D. A.; Cramer, C. J.; Truhlar, D. G. *J. Chem. Phys.* **1999**, *110*, 5503.

(28) Chuang, Y.-Y.; Radhakrishnan, M. L.; Fast, P. L.; Cramer, C. J.; Truhlar, D. G. *J. Phys. Chem. A* **1999**, *103*, 4893.

(29) Fang, Y.; Gao, Y.; Ryberg, P.; Eriksson, J.; Kolodziejska-Huben, M.; Dybala-Defratyka, A.; Madhavan, S.; Danielsson, R.; Paneth, P.; Matsson, O.; Westaway, K. C. *Chem. Eur. J.* **2003**, *9*, 2696.

(30) Dybała-Defratyka, A.; Rostkowski, M.; Matsson, O.; Westaway, K. C.; Paneth, P. *J. Org. Chem.* **2004**, *69*, 4900.

(31) Matsson, O.; Dybala-Defratyka, A.; Rostkowski, M.; Paneth, P.; Westaway, K. C. *J. Org. Chem.* **2005**, *70*, 4022.

(32) Fang, Y.; MacMillar, S.; Eriksson, J.; Kołodziejska-Huben, M.; Dybała-Defratyka, A.; Paneth, P.; Matsson, O.; Westaway, K. C. *J. Org. Chem.* **2006**, *71*, 4742.

(33) Zhao, Y.; Truhlar, D. G. *J. Chem. Phys.* **2006**, *125*, 194101.

(34) Lynch, B. J.; Zhao, Y.; Truhlar, D. G. *J. Phys. Chem. A* **2005**, *109*, 1643.

(35) Marenich, A. V.; Olson, R. M.; Kelly, C. P.; Cramer, C. J.; Truhlar, D. G. *J. Chem. Theory Comput.* **2007**, *3*, 2011.

(36) Olson, R. M.; Marenich, A. V.; Cramer, C. J.; Truhlar, D. G. *J. Chem. Theory Comput.* **2007**, *3*, 2046.

(37) Zhao, Y.; Truhlar, D. G. *MN-GFM-version 3.0*; University of Minnesota: Minneapolis, 2006.

(38) (a) Xidos, J. D.; Li, J.; Hawkins, G. D.; Winget, P.; Zhu, T.; Rinaldi, D.; Liotard, D. A.; Cramer, C. J.; Truhlar, D. G.; Frisch, M. J. *MN-GSM-version 99.8*; University of Minnesota, Minneapolis, 2001. (b) Olson, R. M.; Marenich, A. V.; Chamberlin, A. C.; Kelly, C. P.; Thompson, J. D.; Xidos, J. D.; Li, J.; Hawkins, G. D.; Winget, P.; Zhu, T.; Rinaldi, D.; Liotard, D. A.; Cramer, C. J.; Truhlar, D. G.; Frisch, M. J. *MN-GSM-2008*; University of Minnesota: Minneapolis, 2008.

(39) Frisch, M. J.; Trucks, G. W.; Schlegel, H. B.; Scuseria, G. E.; Robb, M. A.; Cheeseman, J. R.; Montgomery, J. A., Jr.; Vreven, T.; Kudin, K. N.; Burant, J. C.; Millam, J. M.; Iyengar, S. S.; Tomasi, J.; Barone, V.; Mennucci, B.; Cossi, M.; Scalmani, G.; Rega, N.; Petersson, G. A.; Nakatsuji, H.; Hada, M.; Ehara, M.; Toyota, K.; Fukuda, R.; Hasegawa, J.; Ishida, M.; Nakajima, T.; Honda, Y.; Kitao, O.; Nakai, H.; Klene, M.; Li, X.; Knox, J. E.; Hratchian, H. P.; Cross, J. B.; Bakken, V.; Adamo, C.; Jaramillo, J.; Gomperts, R.; Stratmann, R. E.; Yazyev, O.; Austin, A. J.; Cammi, R.; Pomelli, C.; Ochterski, J. W.; Ayala, P. Y.; Morokuma, K.; Voth, G. A.; Salvador, P.; Dannenberg, J. J.; Zakrzewski, V. G.; Dapprich, S.; Daniels, A. D.; Strain, M. C.; Farkas, O.; Malick, D. K.; Rabuck, A. D.; Raghavachari, K.; Foresman, J. B.; Ortiz, J. V.; Cui, Q.; Baboul, A. G.; Clifford, S.; Cioslowski, J.; Stefanov, B. B.; Liu, G.; Liashenko, A.; Piskorz, P.; Komaromi, I.; Martin, R. L.; Fox, D. J.; Keith, T.; Al-Laham, M. A.; Peng, C. Y.; Nanayakkara, A.; Challacombe, M.; Gill, P. M. W.; Johnson, B.; Chen, W.; Wong, M. W.; Gonzalez, C.; Pople, J. A. *Gaussian 03*; Gaussian, Inc.: Wallingford, CT, 2004.

(40) Garrett, B. C.; Truhlar, D. G. *J. Chem. Phys.* **1979**, *70*, 1593.

(41) Garrett, B. C.; Truhlar, D. G. *J. Am. Chem. Soc.* **1979**, *101*, 4534.

(42) Truhlar, D. G.; Garrett, B. C. *Acc. Chem. Res.* **1980**, *13*, 440.

(43) Garrett, B. C.; Truhlar, D. G.; Grev, R. S.; Magnuson, A. W. *J. Phys. Chem.* **1980**, *84*, 1730.

(44) Truhlar, D. G.; Isaacson, A. D.; Garrett, B. C. In *Theory of Chemical Reaction Dynamics*; Baer, M., Ed.; CRC Press: Boca Raton, FL, 1985; Vol. 4, p 65.

(45) Truhlar, D. G.; Garrett, B. C. *J. Chim. Phys.* **1987**, *84*, 365.

(46) Liu, Y.-P.; Lynch, G. C.; Truong, T. N.; Lu, D.-h.; Truhlar, D. G.; Garrett, B. C. *J. Am. Chem. Soc.* **1993**, *115*, 2408.

(47) Truhlar, D. G.; Liu, Y.-P.; Schenter, G. K.; Garrett, B. C. *J. Phys. Chem.* **1994**, *98*, 8396.

(48) Baldridge, K. K.; Gordon, M. S.; Steckler, R.; Truhlar, D. G. *J. Phys. Chem.* **1989**, *93*, 5107.

(49) Gonzàlez-Lafont, A.; Truong, T. N.; Truhlar, D. G. *J. Phys. Chem.* **1991**, *95*, 4618.

(50) Truhlar, D. G. In *The Reaction Path in Chemistry; Understanding Chemical Reactivity Series Vol. 16*; Heidrich, D., Ed.; Kluwer: Dordrecht, 1995; p 229.

(51) Corchado, J. C.; Coitiño, E. L.; Chuang, Y.-Y.; Fast, P. L.; Truhlar, D. G. *J. Phys. Chem. A* **1998**, *102*, 2424.

(52) Corchado, J. C.; Chuang, Y.-Y.; Coitiño, E. L.; Ellingson, B. A.; Zheng, J.; Truhlar, D. G. *Gaussrate-version 9.7*; University of Minnesota: Minneapolis, U.S.A., 2007.

(53) Corchado, J. C.; Chuang, Y.-Y.; Fast, P. L.; Hu, W.-P.; Liu, Y.-P.; Lynch, G. C.; Nguyen, K. A.; Jackels, C. F.; Ramos, A. F.; Ellingson, B. A.; Lynch, B. J.; Zheng, J.; Melissas, V. S.; Villa, J.; Rossi, I.; Coitino, E. L.; Pu, J.; Albu, T. V.; Steckler, R.; Garrett, B. C.; Isaacson, A. D.; Truhlar, D. G. *Polyrate-version 9.7*; University of Minnesota: Minneapolis, U.S.A., 2007.

(54) Lu, D.-h.; Truong, T. N.; Melissas, V. S.; Lynch, G. C.; Liu, Y.-P.; Garrett, B. C.; Steckler, R.; Isaacson, A. D.; Rai, S. N.; Hancock, G. C.; Lauderdale, J. G.; Joseph, T.; Truhlar, D. G. *Comput. Phys. Commun.* **1992**, *71*, 235.

(55) Fast, P. L.; Corchado, J. C.; Truhlar, D. G. *J. Chem. Phys.* **1998**, *109*, 6237.

(56) Fast, P. L.; Truhlar, D. G. *J. Chem. Phys.* **1998**, *109*, 3721.

(57) Gandler, J. R.; Jencks, W. P. *J. Am. Chem. Soc.* **1982**, *104*, 1937.

(58) Jia, Z. S.; Rudzinski, J.; Paneth, P.; Thibblin, A. *J. Org. Chem.* **2002**, *67*, 177.

(59) Mayer, I. *Chem. Phys. Lett.* **1983**, *97*, 270. Addendum: **1985**, *117*, 396.

(60) Johnston, H. S. *Adv. Chem. Phys.* **1960**, *3*, 131.

(61) Albery, W. J.; Kreevoy, M. M. *Adv. Phys. Org. Chem.* **1978**, *16*, 87.

(62) Johnston, H. S.; Parr, C. *J. Am. Chem. Soc.* **1963**, *85*, 2544.

(63) Bernasconi, C. F. *Acc. Chem. Res.* **1992**, *25*, 9.

(64) Thibblin, A.; Ahlberg, P. *J. Am. Chem. Soc.* **1977**, *99*, 7926.

(65) Saunders, W. H., Jr. *Chem. Scr* **1975**, *8*, 27.

(66) Saunders, W. H., Jr. *J. Am. Chem. Soc.* **1985**, *107*, 164.

(67) Melander, L.; Saunders, W. H., Jr. *Reaction Rates of Isotopic Molecules*; Wiley and Sons: New York, 1980.

CT800345J